PHOTONICS Research

PbS quantum dots as a saturable absorber for ultrafast laser

LING YUN,[1,†] YANG QIU,[1,†] CONGHAO YANG,[1] JIE XING,[1] KEHAN YU,[1,*] XIANGXING XU,[2,3] AND WEI WEI[1]

[1]College of Electronic and Optical Engineering & College of Microelectronics, Nanjing University of Posts and Telecommunications, Nanjing 210046, China
[2]Jiangsu Key Laboratory of Biofunctional Materials, School of Chemistry and Materials Science, Nanjing Normal University, Nanjing 210046, China
[3]e-mail: xuxx@njnu.edu.cn
*Corresponding author: kehanyu@njupt.edu.cn

Received 23 July 2018; revised 31 August 2018; accepted 11 September 2018; posted 13 September 2018 (Doc. ID 340424); published 16 October 2018

Low-dimensional nanomaterials, owing to their unique and versatile properties, are very attractive for enormous electronic and optoelectronic applications. PbS quantum dots (QDs), characterized by a large Bohr radius and size-tunable bandgap, are especially interesting for photonic applications in the near-infrared region. Here, oleic acid capped colloidal PbS QDs as a saturable absorber are investigated for ultrashort-pulse generation. The PbS QDs exhibit outstanding nonlinear saturable absorption properties at 1550 nm: a modulation depth up to 44.5% and a thermal damage threshold larger than 30 mJ/cm^2. By incorporating PbS QDs into a fiber laser, a transform-limited soliton pulse as short as 559 fs with a bandwidth of 4.78 nm is realized at 1563 nm. Numerous applications may benefit from the nonlinear saturable absorption properties of PbS QDs, such as near-infrared pulsed lasers and modulators.

https://doi.org/10.1364/PRJ.6.001028

1. INTRODUCTION

Ultrafast pulsed lasers that generate picosecond to femtosecond optical pulses have been extensively investigated in the fields of medicine, frequency combs, materials processing, and telecommunication [1–4]. Currently, the most-widely used ultrashort pulse laser adopts a passive mode-locking technique, which uses a nonlinear optical element called a saturable absorber (SA) to transform the continuous wave into optical pulses [5–8]. Key demands for SAs are broad bandwidth, fast charge carrier relaxation, large modulation depth, high thermal damage threshold, and simple fabrication and integration into an optical fiber system [9–13].

Low-dimensional nanomaterials have attracted tremendous interest from the applied physics community due to their excellent optoelectronic features [14–18]. Owing to short recovery time and high third-order nonlinear susceptibility, one-dimensional (1D) carbon nanotubes and two-dimensional (2D) graphene and graphene-like materials with ultrashort pulse generation in extremely wide wavelength range have been discovered one after another in the past few years [19–23]. Among these SAs, the main challenge is that the fast charge carrier relaxation, large modulation depth, and high damage threshold usually cannot be endued simultaneously on an individual material [24–28]. Therefore, it is necessary to find a novel SA that can overcome all the above challenges and provide saturable absorption over a wider wavelength range.

PbS quantum dots (QDs) have been widely researched due to their tunable optical properties via control of size, structure, and composition [29,30]. Given to the large exciton Bohr radius (18 nm), narrow bandgap energy (0.41 eV for bulk material), and quantum confinement effect, adjustable absorption of PbS QDs over the entire near-infrared (NIR) spectral range can be easily achieved [31], resulting in the advancement of fascinating applications as transistors, photodetectors, and photovoltaic cells [29,32,33]. In the field of nonlinear saturable absorption, Asunskis *et al.* revealed that nonlinear optical absorption of PbS QDs depended on their surface properties [34]. Later, a 2.6-ps pulse at around 1 μm with an output power of 250 mW was observed in PbS QD-doped glass SAs [35]. Gumenyuk *et al.* demonstrated a vector soliton fiber laser centered at 2 μm with a modulation depth >40% [36]. The generation of transform-limited fs optical pulses with QDs was predicted almost two decades ago [37]; however, experimental study on PbS QD mode-locked fs fiber lasers is still rarely reported.

Here, we demonstrate saturable absorption of PbS QDs and generation of a high-power ultrafast-pulse erbium-doped fiber (EDF) laser. Results show a nonlinear saturable absorption feature at 1550 nm with modulation depth up to 44.5%. In a PbS

QD-mode-locked fiber laser, a transform-limited soliton pulse as short as 559 fs is delivered at 1563 nm with a spectral bandwidth of 4.78 nm, and the thermal damage threshold of the PbS QDs is larger than 30 mJ/cm^2.

2. PREPARATION AND CHARACTERIZATION OF THE PbS QD SA

The PbS QDs were prepared by a modified hot-injection method described elsewhere [38,39]. Briefly, PbO, oleic acid, and 1-octadecene were loaded in a flask in vacuum at 120°C to obtain a transparent solution. The S-precursor was prepared by adding S to oleylamine at 120°C in vacuum. Then the S-precursor was quickly injected in and let react for 30 s under argon atmosphere. The reaction mixture was cooled in an ice-water bath [40]. The PbS QDs were separated with ethanol by centrifugation of the reaction solution at 12,000 r/min for 3 min. The precipitated PbS QDs were redispersed in cyclohexane forming a long-term stable colloidal solution [40].

Under a transmission electron microscope (TEM), well-dispersed QDs with uniform size were observed, as illustrated in Fig. 1(a). According to statistical analysis on 515 PbS QDs in the TEM image, the average diameter of the QDs was about 5.7 ± 0.5 nm, as described in the size distribution histogram in Fig. 1(b).

The fiber-based PbS QD SA was fabricated by drop-cast of the as-prepared colloidal QDs on the fiber connector end using a 1-mL syringe, followed by slow evaporation under ambient temperature and pressure. This scheme overcomes the mechanical damage and guarantees high-optical-power-induced thermal damage. Linear absorption of PbS QDs is measured by a spectrophotometer. As demonstrated in Fig. 2(a), the significant absorption peak appears at about 1.5 μm, which corresponds to the PbS QDs' first excitonic absorption state in the strong quantum confinement regime [37].

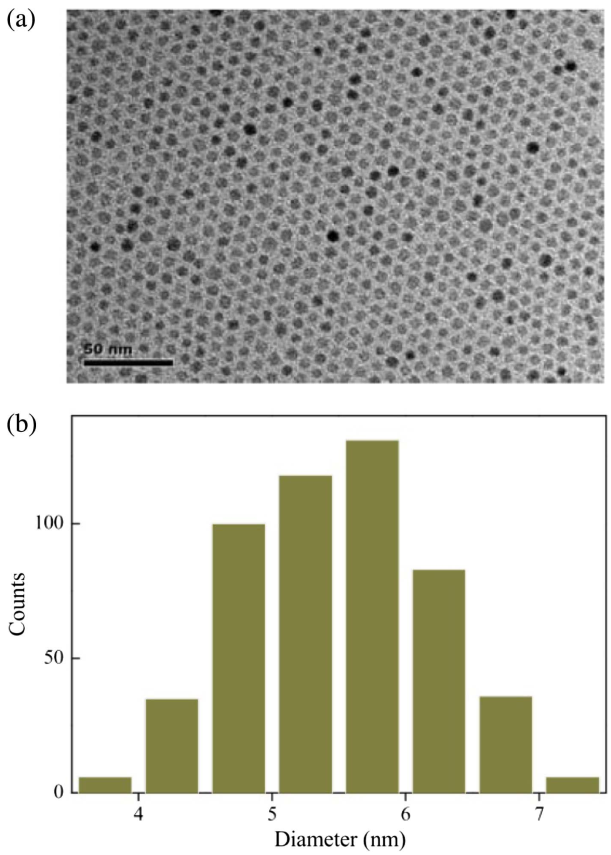

Fig. 1. (a) TEM image and (b) corresponding size distribution histogram of PbS QDs.

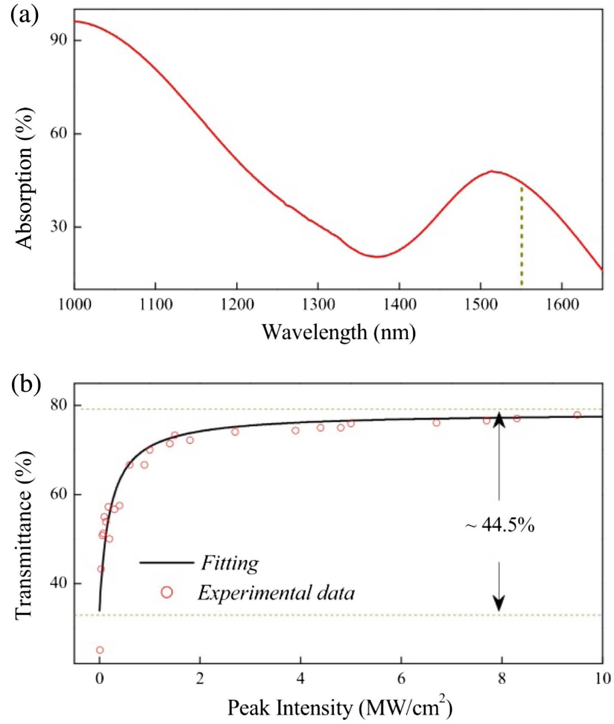

Fig. 2. (a) Linear absorption spectrum of the PbS QDs and (b) nonlinear transmission curve of the PbS QD-based SA.

The nonlinear saturable absorption characteristic of PbS QDs was assessed using the twin-detector measurement technique [41]. The incident optical soliton was generated by a nanotube-mode-locked ultrafast laser source (pulse width 735 fs, fundamental repetition rate 18.8 MHz, central wavelength 1550 nm). We used an attenuator and an amplifier to adjust pulse intensity. Then, the incident optical soliton was equally separated, and the PbS QD SA device was inserted into one of the two branches. The power meter recorded the relationship between incident pump power and average output power. Figure 2(b) shows the saturable absorption characteristic of the PbS QDs at the telecommunication band. According to a two-level model with SA, the solid curve is fitted to the experimental results [42]. The modulation depth of PbS QDs is given as 44.5%, which is comparable to those of most 1D and 2D materials.

3. FIBER SOLITON LASER BASED ON THE PbS QD SA

Figure 3 shows the setup of the fiber laser, and the inset is a digital photograph of the PbS QDs mode locker. The laser consists of an EDF with a length of ~3 m and a dispersion

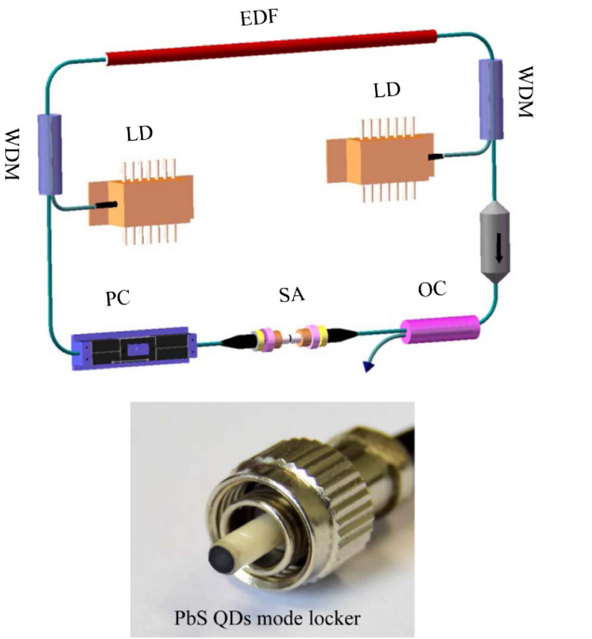

Fig. 3. PbS QD mode-locked laser setup. Inset: digital photograph of the PbS QD mode locker fabricated on the fiber connector end.

parameter D of −16 ps/(nm · km), and a standard single-mode fiber (SMF) with a length of ∼12 m and a dispersion parameter D of 17 ps/(nm · km). The total length of the resonator is ∼15 m, and net dispersion is about −0.2 ps^2. The PbS QD SA fabricated on the fiber connector end is used as a mode-locked element to generate ultrashort pulses. A polarization-insensitive isolator (PI-ISO) guarantees unidirectional traveling waves, and an optical coupler (OC) with 10% output ratio is used to output optical signals. Two 980-nm laser diodes (LDs) with maximum output power of 1 W are used as pump sources and are coupled into the resonator through two 980/1550-nm wavelength division multiplexers (WDMs).

Stable single-pulse mode locking was achieved when the pump power was increased to $P = 50$ mW. As shown in Fig. 4(a), the output spectrum exhibits symmetrically Kelly sidebands, which confirm that it is a conventional soliton [43,44]. The center wavelength is ∼1563 nm, and the 3-dB bandwidth is ∼4.78 nm, respectively. Figure 4(b) illustrates the autocorrelation curve of the conventional soliton and gives a pulse duration of ∼559 fs by fitting with a $sech^2$ function. To our knowledge, it is the first report of a fs pulse in fiber lasers based on a PbS QD SA.

The corresponding time-bandwidth product is 0.33, indicating that the output pulse has no chirp. The oscilloscope trace in Fig. 4(c) shows that pulse intensity is equal, and the pulse interval is ∼71 ns. Figure 4(d) presents the radio frequency spectrum recorded at a span of 100 Hz with a resolution of 1 Hz. The fundamental repetition rate is given as ∼13.9 MHz, which coincides with the cavity length. No radio frequency spectrum modulation is observed over a wide span of 500 MHz, as shown in the inset in Fig. 4(d), indicating no Q-switching instabilities [45]. The signal-to-noise ratio is

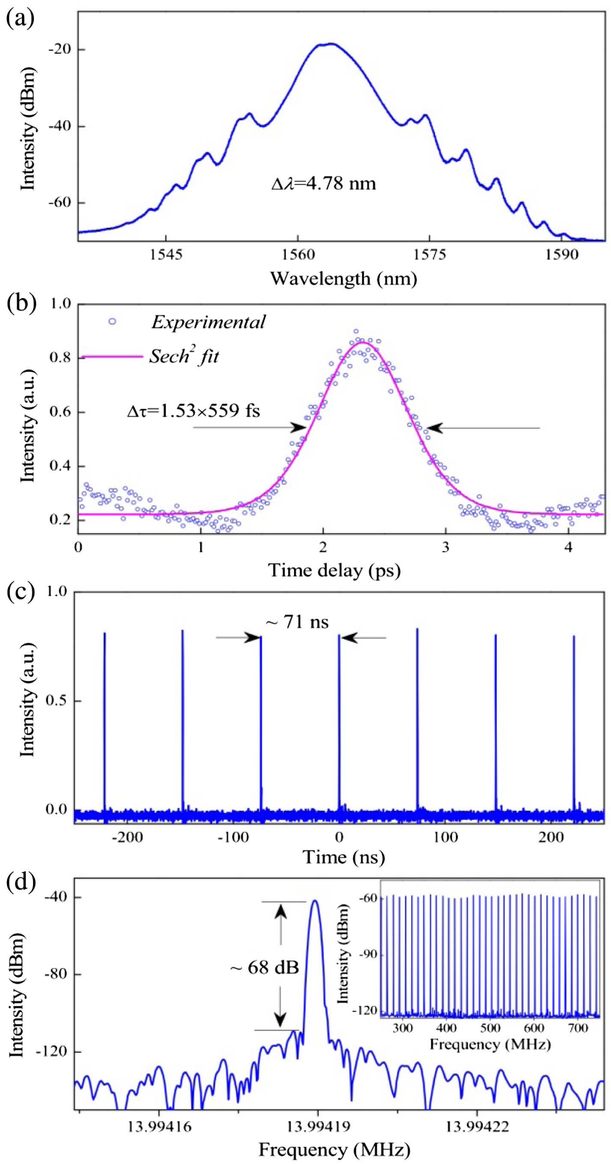

Fig. 4. Mode-locked pulse characteristics. (a) Spectrum, (b) autocorrelation trace, (c) pulse train, and (d) radio frequency spectrum.

greater than 60 dB, indicating that the PbS QD mode-locked fiber laser has good stability.

Moreover, the PbS QD-based SA exhibits excellent thermal stability. Figure 5(a) shows that the average output power of the mode-locked fiber laser increases almost linearly with pump power. An average output power of 23.5 mW is achieved with maximum available pump power of 1 W. Therefore, the thermal damage threshold of PbS QDs must be higher than 30 mJ/cm^2. Figure 5(b) shows the corresponding output spectra at different pump powers. The output spectra remain almost unchanged, indicating stable mode-locked operation states at the available pump powers. Experimental results show that PbS QDs have been proved to exhibit distinct and complementary saturable absorption properties compared to the mentioned 1D and 2D materials. Due to the PbS QD SA exhibiting an extremely large modulation depth, fast decay time,

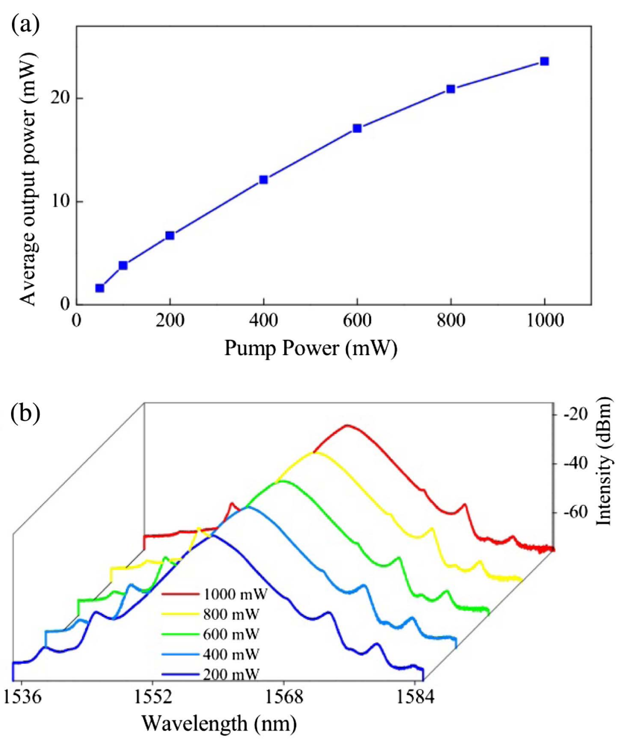

Fig. 5. (a) Average output power versus pump power in mode-locking states and (b) corresponding spectra at different pump powers.

and high thermal damage threshold, it may benefit applications in the fields of high-power pulsed lasers, materials processing, and modulators.

4. CONCLUSION

In conclusion, we fabricate the PbS QD-based SA by drop-cast of colloidal QDs on the fiber connector end. The modulation depth of the PbS QD SA at 1550 nm is up to 44.5%, and the thermal damage threshold is larger than 30 mJ/cm^2. Soliton mode-locking operation as short as 559 fs is obtained in an EDF laser, which is the shortest pulse among all PbS QD-based SAs reported so far. Our results suggest that PbS QDs show advantages of uniformity, large modulation depth, ultrashort pulse duration, and high damage threshold, and therefore may emerge as a good candidate for ultrafast photonics devices.

Funding. National Natural Science Foundation of China (NSFC) (51572120, 61504064); Natural Science Foundation of Jiangsu Province (BK20150847, BK20161521, BK20170912); Nanjing University of Posts and Telecommunications (NUPT) (NY217129, NY218023).

[†]These authors contributed equally to this work.

REFERENCES

1. U. Keller, “Recent developments in compact ultrafast lasers,” Nature **424**, 831–838 (2003).
2. M. E. Fermann and I. Hartl, “Ultrafast fibre lasers,” Nat. Photonics **7**, 868–874 (2013).
3. X. M. Liu, Y. D. Cui, D. D. Han, X. K. Yao, and Z. P. Sun, “Distributed ultrafast fibre laser,” Sci. Rep. **5**, 9101 (2015).
4. D. Y. Tang, H. Zhang, L. M. Zhao, and X. Wu, “Observation of high-order polarization-locked vector solitons in a fiber laser,” Phys. Rev. Lett. **101**, 153904 (2008).
5. X. M. Liu, H. R. Yang, Y. D. Cui, G. W. Chen, Y. Yang, X. Q. Wu, X. K. Yao, D. D. Han, X. X. Han, C. Zeng, J. Guo, W. L. Li, G. Cheng, and L. M. Tong, “Graphene-clad microfibre saturable absorber for ultrafast fibre lasers,” Sci. Rep. **6**, 26024 (2016).
6. S. B. Lu, L. L. Miao, Z. N. Guo, X. Qi, C. J. Zhao, H. Zhang, S. C. Wen, D. Y. Tang, and D. Y. Fan, “Broadband nonlinear optical response in multi-layer black phosphorus: an emerging infrared and mid-infrared optical material,” Opt. Express **23**, 11183–11194 (2015).
7. C. Zhao, H. Zhang, X. Qi, Y. Chen, Z. T. Wang, S. C. Wen, and D. Y. Tang, “Ultra-short pulse generation by a topological insulator based saturable absorber,” Appl. Phys. Lett. **101**, 211106 (2012).
8. Z. Luo, M. Zhou, J. Weng, G. Huang, H. Xu, C. Ye, and Z. Cai, “Graphene-based passively *Q*-switched dual wavelength erbium-doped fiber laser,” Opt. Lett. **35**, 3709–3711 (2010).
9. T. Hasan, Z. Sun, F. Wang, F. Bonaccorso, P. H. Tan, A. G. Rozhin, and A. C. Ferrari, “Nanotube-polymer composites for ultrafast photonics,” Adv. Mater. **21**, 3874–3899 (2009).
10. L. M. Zhao, D. Y. Tang, H. Zhang, X. Wu, and N. Xiang, “Soliton trapping in fiber lasers,” Opt. Express **16**, 9528–9533 (2008).
11. G. Sobon, J. Sotor, and K. M. Abramski, “Passive harmonic mode-locking in Er-doped fiber laser based on graphene saturable absorber with repetition rates scalable to 2.22 GHz,” Appl. Phys. Lett. **100**, 161109 (2012).
12. L. L. Gui, X. S. Xiao, and C. X. Yang, “Observation of various bound solitons in a carbon-nanotube-based erbium fiber laser,” J. Opt. Soc. Am. B **30**, 158–164 (2013).
13. Z. Sun and H. Chang, “Graphene and graphene-like two-dimensional materials in photodetection: mechanisms and methodology,” ACS Nano **8**, 4133–4156 (2014).
14. A. Martinez and Z. Sun, “Nanotube and graphene saturable absorbers for fibre lasers,” Nat. Photonics **7**, 842–845 (2013).
15. Y. F. Song, H. Zhang, L. M. Zhao, D. Y. Shen, and D. Y. Tang, “Coexistence and interaction of vector and bound vector solitons in a dispersion-managed fiber laser mode locked by graphene,” Opt. Express **24**, 1814–1822 (2016).
16. Q. L. Bao, H. Zhang, Y. Wang, Z. H. Ni, Y. L. Yan, Z. X. Shen, K. P. Loh, and D. Y. Tang, “Atomic-layer graphene as a saturable absorber for ultrafast pulsed lasers,” Adv. Funct. Mater. **19**, 3077–3083 (2009).
17. D. Popa, Z. Sun, F. Torrisi, T. Hasan, F. Wang, and A. C. Ferrari, “Sub 200 fs pulse generation from a graphene mode-locked fiber laser,” Appl. Phys. Lett. **97**, 203106 (2010).
18. Z. Sun, T. Hasan, F. Torrisi, D. Popa, G. Privitera, F. Wang, F. Bonaccorso, D. M. Basko, and A. C. Ferrari, “Graphene mode-locked ultrafast laser,” ACS Nano **4**, 803–810 (2010).
19. F. Wang, A. Rozhin, V. Scardaci, Z. Sun, F. Hennrich, I. White, W. Milne, and A. Ferrari, “Wideband-tuneable, nanotube modelocked, fibre laser,” Nat. Nanotechnol. **3**, 738–742 (2008).
20. H. Zhang, D. Y. Tang, L. M. Zhao, Q. L. Bao, and K. P. Loh, “Large energy soliton erbium-doped fiber laser with a graphene-polymer composite mode locker,” Appl. Phys. Lett. **95**, 141103 (2009).
21. H. Zhang, S. B. Lu, J. Zheng, J. Du, S. C. Wen, D. Y. Tang, and K. P. Loh, “Molybdenum disulfide MoS_2 as a broadband saturable absorber for ultra-fast photonics,” Opt. Express **22**, 7249–7260 (2014).
22. J. Sotor, G. Sobon, W. Macherzynski, P. Paletko, and K. M. Abramski, “Black phosphorus saturable absorber for ultrashort pulse generation,” Appl. Phys. Lett. **107**, 051108 (2015).
23. D. Mao, B. Jiang, X. Gan, C. Ma, Y. Chen, C. Zhao, H. Zhang, J. Zheng, and J. Zhao, “Soliton fiber laser mode locked with two types of film-based Bi_2Te_3 saturable absorbers,” Photon. Res. **3**, A43–A46 (2015).
24. Y. Xu, W. Wang, Y. Ge, H. Guo, X. Zhang, S. Chen, Y. Deng, Z. Lu, and H. Zhang, “Stabilization of black phosphorous quantum dots in PMMA nanofiber film and broadband nonlinear optics and ultrafast photonics application,” Adv. Funct. Mater. **27**, 1702437 (2017).
25. Z. C. Luo, M. Liu, H. Liu, X. W. Zheng, A. P. Luo, C. J. Zhao, H. Zhang, S. C. Wen, and W. C. Xu, “2 GHz passively harmonic mode-locked fiber laser by a microfiber-based topological insulator saturable absorber,” Opt. Lett. **38**, 5212–5215 (2013).

26. Y. F. Song, Z. M. Liang, X. T. Jiang, Y. X. Chen, Z. J. Li, L. Lu, Y. Q. Ge, K. Wang, J. L. Zheng, S. B. Lu, J. H. Ji, and H. Zhang, "Few-layer antimonene decorated microfiber: ultra-short pulse generation and all-optical thresholding with enhanced long term stability," 2D Mater. **4**, 045010 (2017).
27. Q. L. Bao, H. Zhang, Z. H. Ni, Y. Wang, L. Polavarapu, Z. X. Shen, Q. H. Xu, D. Y. Tang, and K. P. Loh, "Monolayer graphene as a saturable absorber in a mode-locked laser," Nano Res. **4**, 297–307 (2011).
28. H. Mu, Z. Wang, J. Yuan, S. Xiao, C. Chen, Y. Chen, Y. Chen, J. Song, Y. Wang, Y. Xue, H. Zhang, and Q. L. Bao, "Graphene-Bi_2Te_3 heterostructure as saturable absorber for short pulse generation," ACS Photon. **2**, 832–841 (2015).
29. E. U. Rafailov, M. A. Cataluna, and W. Sibbett, "Mode-locked quantum-dot lasers," Nat. Photonics **1**, 395–401 (2007).
30. T. Y. Liu, M. Li, J. Ouyang, M. Zaman, R. Wang, X. Wu, C. Yeh, Q. Lin, B. Yang, and K. Yu, "Non-injection and low-temperature approach to colloidal photoluminescent PbS nanocrystals with narrow bandwidth," J. Phys. Chem. C **113**, 2301–2308 (2009).
31. I. Moreels, K. Lambert, and D. Smeets, "Size-dependent optical properties of colloidal PbS quantum dots," ACS Nano **3**, 3023–3030 (2009).
32. S. A. McDonald, P. W. Cyr, L. Levina, and E. H. Sargent, "Photoconductivity from PbS-nanocrystal/semiconducting polymer composites for solution-processible, quantum-size tunable infrared photodetectors," Appl. Phys. Lett. **85**, 2089–2091 (2004).
33. S. A. Mcdonald, G. Konstantatos, S. G. Zhang, P. W. Cyr, E. J. D. Klem, L. Levina, and E. H. Sargent, "Solution-processed PbS quantum dot infrared photodetectors and photovoltaics," Nat. Mater. **4**, 138–142 (2005).
34. D. J. Asunskis, I. L. Bolotin, and L. Hanley, "Nonlinear optical properties of PbS nanocrystals grown in polymer solutions," J. Phys. Chem. C **112**, 9555–9558 (2008).
35. A. A. Lagatsky, A. M. Malyarevich, V. G. Savitski, M. S. Gaponenko, K. V. Yumashev, A. A. Zhilin, C. T. A. Brown, and W. Sibbett, "PbS quantum-dot-doped glass for efficient passive mode locking in a cw Yb:KYW laser," IEEE Photon. Technol. Lett. **18**, 259–261 (2006).
36. R. Gumenyuk, M. S. Gaponenko, K. V. Yumashev, A. A. Onushchenko, and O. G. Okhotnikov, "Vector soliton bunching in thulium-holmium fiber laser mode-locked with PbS quantum-dot-doped glass absorber," IEEE J. Quantum Electron. **48**, 903–907 (2012).
37. K. Wundke, S. Pötting, J. Auxier, A. Schülzgen, N. Peyghambarian, and N. F. Borrelli, "PbS quantum-dot-doped glasses for ultrashort-pulse generation," Appl. Phys. Lett. **76**, 10–12 (2000).
38. J. Joo, H. B. Na, T. Yu, J. H. Yu, Y. W. Kim, F. X. Wu, J. Z. Zhang, and T. Hyeon, "Generalized and facile synthesis of semiconducting metal sulfide nanocrystals," J. Am. Chem. Soc. **125**, 11100–11105 (2003).
39. M. A. Hines and G. D. Scholes, "Colloidal PbS nanocrystals with size-tunable near-infrared emission: observation of post-synthesis self-narrowing of the particle size distribution," Adv. Mater. **15**, 1844–1849 (2003).
40. J. Lu, X. Sheng, G. Tong, Z. Yu, X. Sun, L. Yu, X. Xu, J. Wang, J. Xu, Y. Shi, and K. Chen, "Ultrafast solar-blind ultraviolet detection by inorganic perovskite CsPbX3 quantum dots radial junction architecture," Adv. Mater. **29**, 1700400 (2017).
41. C. H. Yang, L. Yun, Y. Qiu, H. Q. Dai, D. T. Zhu, Z. J. Zhu, Z. X. Zhang, K. H. Yu, and W. Wei, "Direct growth of a graphitic nano-layer on optical fibers for ultra-fast laser application," RSC Adv. **7**, 52261–52265 (2017).
42. X. M. Liu, D. D. Han, Z. P. Sun, C. Zeng, H. Lu, D. Mao, Y. D. Cui, and F. Q. Wang, "Versatile multi-wavelength ultrafast fiber laser mode-locked by carbon nanotubes," Sci. Rep. **3**, 2718 (2013).
43. L. Yun, "Generation of vector dissipative and conventional solitons in large normal dispersion regime," Opt. Express **25**, 18751–18759 (2017).
44. D. Mao, B. Du, D. Yang, S. Zhang, Y. Wang, W. Zhang, X. She, H. Cheng, H. Zeng, and J. Zhao, "Nonlinear saturable absorption of liquid-exfoliated molybdenum/tungsten ditelluride nanosheets," Small **12**, 1489–1497 (2016).
45. L. Yun, "Black phosphorus saturable absorber for dual-wavelength polarization-locked vector soliton generation," Opt. Express **25**, 32380–32385 (2017).